



# IDH-mutant Glioma Subtypes Classification Using Unsupervised Dimensionality Reduction of MRI Biomarkers

**Nazanin Maleki, MD**, Research Fellow, Radiology, The Children's Hospital of Philadelphia

Klara Willms, MD; Tal Zeevi, PhD; Sahil Chadha, MD; Marc von Reppert, MD; Leon Jekel, MD; Jan Lost, MD; Sarah Merkaj, MD; Niklas Tilmanns, MD; Mariam Aboian, MD, PhD

## Introduction

IDH-mutant glioma share many similarities on MRI and histopathology but have distinct differences in their survival based on their molecular subtypes. Radiomic biomarkers provide insights into glioma imaging phenotypes that may not appear in clinical evaluation. This study aimed to evaluate whether MRI-based biomarkers of IDH-mutant gliomas can differentiate 2021 CNS5 WHO classification molecular subtypes and identify distinct patterns of overall survival.

## Hypothesis

To explore the use of radiomic biomarkers to classify IDH-mutant gliomas subtype.

## Methods

We included 179 adult patients with IDH-mutant, 1p/19q co-deleted oligodendrogliomas (WHO CNS5 grade 2-3) and IDH-mutant, non co-deleted astrocytoma (WHO CNS5 grades 2-4) with pre-treatment MRI on FLAIR, T1 post-contrast and T2. Segmentations were performed using a UNETR algorithm trained on the BRaTS 2021 dataset and manual modification. M=94 texture biomarkers were extracted from the segmentation region of each scan using the PyRadiomics 3.1.0 pipeline (s. Figure 1). Dimensionality reduction techniques (PCA, t-SNE, UMAP, and PHATE) were employed to the radiomic biomarkers of (i) FLAIR; (ii) FLAIR and T1 post-contrast imaging (PGGE/PGSE); (iii) incorporating one-hot encoded lesion location information; and (iv) FLAIR and T2 imaging. K-Means clustering was used to identify relevant clinical clusters in the reduced space.

## Results

Figure 2 illustrates subtype distribution across K-Means clusters. (i) For FLAIR-based biomarkers, all dimensionality reduction techniques produced identical distributions between clusters B and C. The highest representations included 27.1% oligodendroglioma, grade 2, 24.8% astrocytoma, grade 2, and 19.4% oligodendroglioma in one cluster, and 31.1% astrocytoma, grade 2, 24.4% oligodendroglioma, grade 3, and 17.8% oligodendroglioma, grade 2 in the other. (ii) Adding radiomic features from T1 post-contrast, PCA differed: Cluster A had 46.7% astrocytoma, grade 2, versus 37.8% in Cluster B and 23.2% in Cluster C. TSNE, PHATE, and UMAP showed 46.2% astrocytoma, grade 2 in Cluster B, and 34.6% in Cluster C. (iv) Adding T2/FLAIR mismatch sign revealed no significant distribution differences: 20.9% positive mismatch in Cluster A

and 12.8% in Cluster B. Kaplan-Meier survival analysis of UMAP clusters (log-rank test) showed no significant survival differences:  $p=0.781$  (FLAIR),  $p=0.054$  (FLAIR+T1Gd),  $p=0.455$  (FLAIR+T2; Figure 3).

## Conclusion

We show that there is a spectrum of imaging features of IDH-mutant gliomas that have significant overlap on FLAIR and T1 post-contrast imaging, but cluster into two groups only on FLAIR and three clusters when adding T1WI post-gadolinium radiomic features.

## Figure(s)

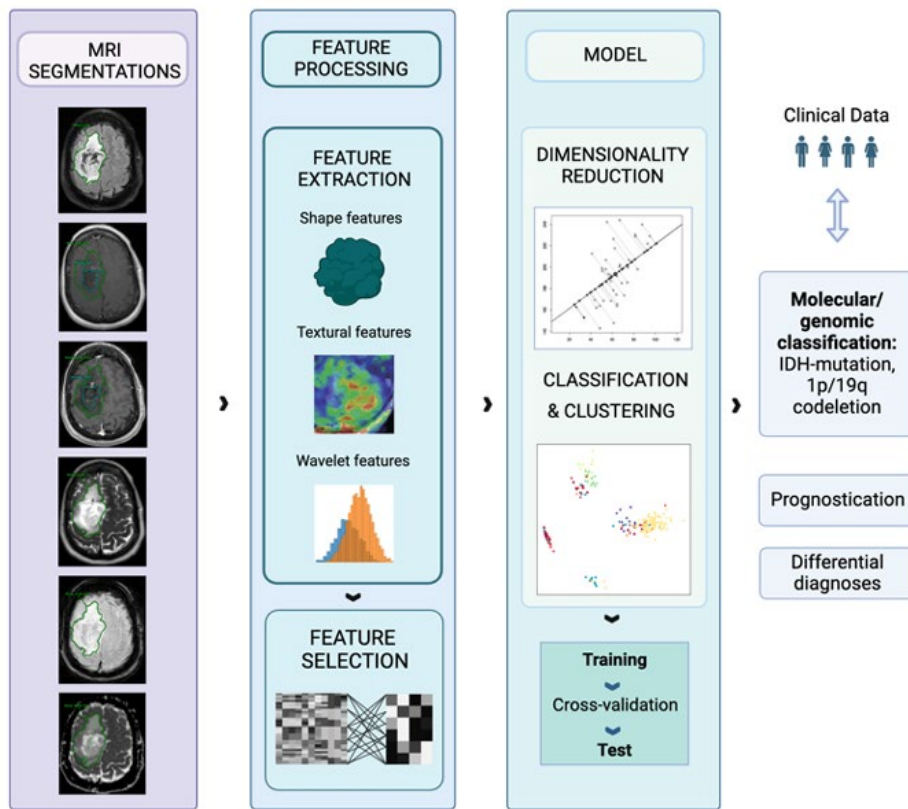


**Figure 1.** Distribution of tumor subtypes across K-Means clusters. (i) For FLAIR-based biomarkers, identical subtype distributions emerged among clusters B and C across all dimensionality reduction techniques. Subtype proportions are shown for each cluster. (ii) PCA analysis incorporating T1 post-contrast features showed Cluster A with 46.7% astrocytoma, grade 2, while Clusters B and C contained 37.8% and 23.2%, respectively. TSNE, PHATE, and UMAP results showed higher astrocytoma, grade 2 representation in Cluster B (46.2%) compared to Cluster C (34.6%). (iv) Adding T2 imaging, no significant differences in T2/FLAIR mismatch sign distribution were observed.

Step	Cluster	PCA					TSNE, PHATE, UMAP				
		AS 2	AS 3	AS 4	OD 2	OD 3	AS 2	AS 3	AS 4	OD 2	OD 3
I)	B	31.1%	11.1%	15.6%	17.8	24.4%	31.1%	11.1%	15.6%	17.8	24.4%
	C	24.8%	18.6%	10.1%	27.1	19.4%	24.8%	18.6%	10.1%	27.1	19.4%
II)	A	46.7%	20.0%	13.3%	13.3%	6.7%	27.8%	22.2%	20.0%	18.9%	11.1%
	B	37.8%	11.1%	8.9%	15.6%	26.7%	46.2%	15.4%	-	15.4%	23.1%
	C	23.2%	18.8%	13.0%	20.3%	24.6%	34.6%	7.7%	19.2%	11.5%	26.9%
III)	See Step II results.										

**Table 1.** Cluster Distributions of Dimensionality Reduction Techniques.

## Keywords

Artificial Intelligence/Machine Learning; Imaging Research